Estrogen Exerts a Spatial and Temporal Influence on Reactive Oxygen Species Generation that Precedes Calcium Uptake in High-Capacity Mitochondria: Implications for Rapid Nongenomic Signaling of Cell Growth†

Jai Parkash, Quentin Felty, and Deodutta Roy*

Department of Environmental and Occupational Health, Robert Stempel School of Public Health, Florida International University, Miami, Florida 33199

Received September 12, 2005; Revised Manuscript Received December 7, 2005

ABSTRACT: Novel findings that emerged from this study underscore the fact that the dynamic nature of mitochondria leads to functional heterogeneity of $[Ca^{2+}]_{mito}$ with respect to estrogen actions in MCF7 cells. We show that estrogen exposure to cells increased $[Ca^{2+}]_{mito}$ in a high-calcium capacity mitochondrial population but not in low-calcium capacity mitochondria. Physiological concentrations of 17β-estradiol (E2) modulated $Ca^{2+}{}_{mito}$ uptake within 90 s. Interestingly, this calcium response lagged behind the induction of mitochondrial reactive oxygen species (mtROS). The rapid induction of $Ca^{2+}{}_{mito}$ in response to E2 and its inhibition by mitochondrial blockers suggest that mitochondria are early nongenomic targets of E2. This suggests that a subpopulation of mitochondria is recruited to respond to new metabolic requirements required by estrogen triggers or, as in this case, E2-induced $Ca^{2+}{}_{mito}$ and/or mtROS promotes oxidative signaling without involving nuclear estrogen receptor signaling. Although the early E2-induced Ca^{2+} did not alter the expression of genes involved in calcium signaling pathways, an intracellular calcium chelator BAPTA-AM and the $Ca^{2+}{}_{mito}$ uniporter blocker ruthenium red prevented E2-induced cell growth. We have shown recently that E2-mediated ROS production controls the promoter activity of cyclin D1 by post-translational modification of calcium sensitive transcription factor CREB. The findings of this study offer a new paradigm that rapid E2-induced changes in mtROS and $Ca^{2+}{}_{mito}$ are involved in cell cycle progression presumably through the control of early cell cycle genes. Targeting mitochondria to disrupt communication between mitochondria and ROS/Ca^{2+} signaling pathways may provide the basis for a novel anticancer strategy for the treatment of estrogen-dependent breast cancer.

Studies of nongenomic estrogen effects have been focused on the plasma membrane estrogen receptor (ER).[1] For instance, estrogen has been shown to rapidly increase the intracellular Ca^{2+} concentration ($[Ca^{2+}]_i$) by initiating a signal through a G protein-coupled membrane ER (*1*, *2*). Recently, we have reported that mitochondria are an important early target of estrogen action. The cross-talk between the cell nucleus and the mitochondria appears to control estrogen-induced signaling involved in cell growth of both normal and malignant cells (*3*). 17β-Estradiol (E2)-induced mitochondrial (mt) reactive oxygen species (ROS) act as signal-transducing messengers that control the G_1-to-S transition of G_0-arrested estrogen-dependent cells (*4*, *5*). Calcium is also a well-established second messenger that has been shown to modulate the early G_1 phase and the G_1-to-S phase boundary of the cell cycle (*6*). A transient increase in the Ca^{2+} concentration within the perinuclear compartment of a dividing cell was followed by an increase in the whole cell's $[Ca^{2+}]_i$ but ceased once cells progressed into the S phase. We previously showed a localization of ROS production in perinuclear mitochondria when cells were exposed to E2; therefore, a potential relationship between perinuclear mtROS and mitochondrial Ca^{2+} ($Ca^{2+}{}_{mito}$) is intriguing because both factors are known to play a role in cell cycle progression. Whether an increase in the level of mtROS in response to E2 precedes an increase in $[Ca^{2+}{}_{mito}]$ or vice versa in response to E2 exposure is not clear.

Phytoestrogens have been shown to activate the mitochondrial Ca^{2+} uniporter (*7*). In addition, Ca^{2+} transport across the mitochondrial inner membrane is facilitated through the Ca^{2+}-induced mitochondrial permeability transition pore (PTP) (*8*) which has also been shown to be modulated by E2 (*9*). During cell activation, mitochondria play an important role in Ca^{2+} homeostasis due to the presence of a fast and specific Ca^{2+} channel in its inner membrane, the mitochondrial Ca^{2+} uniporter. This channel allows mitochondria to buffer local cytosolic $[Ca^{2+}]$ changes and controls the $[Ca^{2+}]_{mito}$, thus modulating processes such as oxidative phosphorylation, cytosolic calcium signaling, and apoptosis (*8*). Previous studies, though few in number,

† This work was supported by NIH Grant ES10851 to D.R.

* To whom correspondence should be addressed: Department of Environmental and Occupational Health, Robert Stempel School of Public Health, Florida International University, 11200 SW 8th St., HLS 591, Miami, FL 33199. E-mail: Droy@fiu.edu. Phone: (305) 348-1694. Fax: (305) 348-4901.

[1] Abbreviations: ER, estrogen receptor; E2, 17β-estradiol; mtROS, mitochondrial reactive oxygen species; $[Ca^{2+}]_{mito}$, mitochondrial Ca^{2+} concentration; $[Ca^{2+}]_i$, intracellular Ca^{2+} concentration; $Ca^{2+}{}_{mito}$, mitochondrial Ca^{2+}; TMRM, tetramethylrhodamine methyl ester; DCFH-DA, 2′,7′-dichlorofluorescein diacetate; DCF, 2′,7′-dichlorofluorescein; $\Delta_\Psi m$, mitochondrial membrane potential.

10.1021/bi051855x CCC: $33.50
Published on Web 02/10/2006

have shown the modulation of mitochondrial calcium in brain cells by E2 exposure (*10*, *11*). More recently, E2 has been shown to modulate mitochondrial calcium uptake in cancer cells (*12*). However, this study was limited in terms of spatial resolution because it measured total Ca^{2+}_{mito} uptake of an E2-treated cell population rather than monitoring Ca^{2+}_{mito} uptake within individual cells. In addition, the reported effects occurred at toxicological concentrations (1−40 μM) of E2 which raises concerns about their physiological significance.

Distinct populations of mitochondria with different biochemical and respiratory properties exist in cells (*13*). Previous studies have failed to identify a differential mitochondrial response after E2 exposure because they did not investigate the spatial distribution of Ca^{2+}_{mito} within the cells. The temporal and spatial regulation of signaling molecules within the cell is critical in the regulation of various cellular functions, and mitochondria play crucial roles in these processes. The aims of this study were (i) to investigate whether E2-induced production of mtROS occurs before Ca^{2+}_{mito} uptake, (ii) to determine the existence of distinct subpopulations of mitochondria with respect to calcium uptake in response to transient (from 1 to 90 min) and extended exposure (up to 72 h) of MCF7 cells to physiological concentrations of estrogen, and (iii) to investigate the biological implications of E2-induced mitochondrial calcium uptake.

MATERIALS AND METHODS

Cell Culture and Chemicals. The MCF7 human breast cancer cell line was obtained from American Type Culture Collection (ATCC, Manassas, VA) and routinely cultured in DMEM/F12 medium without phenol red supplemented with 10% FBS and 1× antibiotic-antimycotic and incubated at 37 °C in 5% CO_2. For experimental purposes, cells were seeded in 10% charcoal-dextran stripped FBS DMEM/F12 medium and allowed to adhere for 24 h on 25 mm diameter coverslips that were placed in a six-well tissue culture plate. After cells reached 50−60% confluency, the culture medium was replaced with serum-free DMEM/F12 and cells were grown for an additional 24 h. Serum deprivation was used to synchronize cells in the G_0/G_1 phase of the cell cycle prior to treatment with 100 pg/mL 17β-estradiol. An equivalent volume of the vehicle [ethyl alcohol, final concentration of 0.02% (v/v)] was used as the control. All chemicals were obtained from Sigma Chemical Co. unless stated otherwise. All tissue culture media were obtained from GIBCO (Invitrogen). All fluorescence indicators were from Molecular Probes (Invitrogen).

Simultaneous Loading of Cells with Rhod-2 and MitoTracker Green. The coverslips containing cells were washed twice with Hank's balanced salt solution (HBSS) and incubated in 2 mL of HBSS per well in a six-well culture plate. A 1 mM stock solution of rhod-2/AM was prepared in DMSO. Similarly, a 1 mM stock solution of MitoTracker Green/FM was made in DMSO and then further diluted to 1 μM in phosphate-buffered saline (PBS). Rhod-2/AM is a fluorescent probe used to measure $[Ca^{2+}]_{mito}$, whereas MitoTracker Green/FM is a fluorescent dye that is used to specifically locate mitochondria. The cells were dual-loaded with 1 μM rhod-2/AM for 15 min in the presence of 0.02% (w/v) Pluronic F-127 (Molecular Probes), a nonionic detergent that disperses hydrophobic fluorescent dyes and aids in the uniform loading of cells with the fluorophore, and this was followed by loading cells with 50 nM MitoTracker Green/FM for an additional 15 min. Therefore, the total incubation period with rhod-2/AM was 30 min. The cells were then washed and incubated with HBSS for 15 min at room temperature to completely hydrolyze rhod-2/AM and MitoTracker Green/FM and thus complete the loading process of both fluorophores.

Determination of $[Ca^{2+}]_{mito}$ by Confocal Microscopy. The confocal images were acquired on a Bio-Rad MRC 1024 laser scanning confocal microscope (Bio-Rad, Hertfordshire, England), and the procedure is described in brief. The coverslip containing rhod-2/AM- and MitoTracker Green/FM-loaded cells was placed in a Narishige micro-incubation chamber (Narishige International USA Inc.) with 1 mL of HBSS. The confocal fluorescence images were recorded at room temperature (25 °C) by using excitation wavelengths of 488 nm for MitoTracker Green and 568 nm for rhod-2. These wavelengths were provided by a krypton−argon laser. The fluorescence emissions were detected in the green and orange-red regions by placing a 522DF32 filter (for the green channel) and a HQ598/40 filter (for orange-red emission) in front of the photomultiplier tubes. The *z*-series scanning was done in increments of 0.5 μm up to a *z*-depth of 10 μm by using a 40× oil immersion objective. The calibration of the fluorescence signals for the determination of $[Ca^{2+}]_{mito}$ was done by adding 5 μM ionomycin to obtain F_{max} (maximum fluorescence intensity) and 20 mM EGTA to obtain F_{min} (minimum fluorescence intensity) at the end of each experiment. The built-in LaserSharp version 3.2 software (Bio-Rad), Confocal Assistant version 4.02 (copyrighted by T. C. Brelje), and Metamorph version 4.17 (Universal Imaging Corp., Westchester, PA) were used for confocal image acquisition and analyses. The results were calculated as described previously (*14*). In brief, $[Ca^{2+}]_{mito} = K_d(F - F_{min})/(F_{max} - F)$, where K_d is the dissociation constant of rhod-2 (a value of 1 μM was used), F_{min} is the minimum fluorescence intensity of the indicator (rhod-2) in the absence of calcium (i.e., upon addition of EGTA), F_{max} is the maximum fluorescence intensity of the calcium-saturated rhod-2 (i.e., upon addition of ionomycin), and F is the intermediate calcium concentrations (i.e., experimental).

Determination of Mitochondrial ROS by Confocal Microscopy. The fluorophores used were 2′,7′-dichlorofluorescin diacetate (DCFH-DA) and Mitotracker Deep Red. The MCF7 cells were grown on 25 mm diameter coverslips as described previously. Each coverslip was removed and placed in a Narishige micro-incubation chamber holder. The cells were washed twice with HBSS and incubated in 1 mL of HBSS. To the cells were added 2 μL of DCFH-DA (1 mM) and 2 μL of Pluronic F-127, and the cells were incubated for 15 min at room temperature. To the cells was added 100 μL of stock Mitotracker Deep Red (1 μM), and cells were incubated for 15 min. Cells were washed three times with HBSS and incubated for an additional 15 min in HBSS followed by treatments. The confocal fluorescence images were scanned at room temperature by using excitation wavelengths of 488 nm for DCF and 647 nm for Mitotracker Deep Red.

cAMP/Ca^{2+} PathwayFinder cDNA Array. Gene expression was assessed using the nonradioactive GEArray Q Series

Kit (SuperArray, Inc., Bethesda, MD) for human cAMP/Ca^{2+} sensitive genes. MCF7 cells were treated with E2 (100 pg/mL) for 6 h. Total RNA was isolated from cells using TRIzol Reagent (Invitrogen). Total RNA was used as the template for cDNA probe synthesis according to the manufacturer's instructions. The GEArray membrane was hybridized with a denatured cDNA probe of the samples overnight, and gene expression was detected by a chemiluminescent reaction mixture exposed to X-ray film. Signals were quantitated by scanning the film with an HP ScanJet, and the intensity value of the spots was obtained using the image analysis program Scanalyze (M. Eisen, Stanford, CA). After intensity values had been obtained, each gene was normalized to the housekeeping gene ribosomal protein L13a (RPL13A) using the GEArrayAnalyzer program (SuperArray, Inc.).

Post-cDNA Array Analysis. cDNA was synthesized by using a standard reverse transcription reaction as described previously (*15*). Real-time PCR was performed in a MJ Research DNA Engine Opticon2 apparatus using the TaqMan Gene Expression Assay (Applied Biosystems) for genes NKIR and TGF b3 with 18S rRNA as the endogenous control. Samples were amplified in triplicate according to the manufacturer's instructions.

Cell Growth. Cell growth was assessed by the sulforhodamine B (SRB) assay as described previously (*16*). Dye intensity was measured at 560 nm (reference λ at 700 nm) on a Tecan Genios plate reader.

BrdUrd Cell Proliferation Assay. MCF7 cells were grown (2500 cells/well) in 96-well plates until they were 50% confluent in 10% FBS DMEM/F12 and serum-starved for 2 days. Cells were then pretreated with either BAPTA-AM (10 μM) or ruthenium red (50 μM) for 30 min followed by treatment with E2 (100 pg/mL) for 48 h. A colorimetric BrdUrd incorporation assay was performed according to the manufacturer's instructions (Roche). The absorbance of the samples was measured in a Tecan Genios instrument at 450 nm (reference λ at 700 nm).

Mitochondrial Membrane Potential ($\Delta\Psi m$) Assay. Cells were seeded (20 000 cells/well) in a 96-well black-walled plate, grown for 1 day in 10% FBS DMEM/F12, and serum-starved for 2 days in DMEM/F12 prior to treatments. Cells were pretreated with BAPTA-AM (20 μM) or ruthenium red (50 μM) for 30 min followed by E2 (100 pg/mL) treatment for an additional 30 min in the standard assay buffer [80 mM NaCl, 75 mM KCl, 25 mM D-glucose, and 25 mM HEPES (pH 7.4)]. Membrane potential was measured by the tetramethylrhodamine methyl ester (TMRM) assay as described previously (*17*). TMRM is a cationic-lipophilic dye that is sequestered in the mitochondrial matrix in amounts that are proportional to the membrane potential. Therefore, measurement of the amount of TMRM fluorescence was used to estimate the $\Delta\Psi m$. In brief, 10 μL of a 1.65 μM TMRM stock was added so the final concentration in wells was 150 nM. After a 5 min incubation at room temperature, cells were washed four times with phosphate-buffered saline (PBS). After washing had been carried out, TMRM fluorescence was read on a Tecan Genios instrument using an excitation wavelength of 530 nm and an emission wavelength of 580 nm.

Statistical Analyses. The data were analyzed for statistical significance by using the Student's *t*-test (SigmaStat, Jandel Scientific Software, San Rafael, CA). ANOVA was used to determine differences between groups.

RESULTS

Effect of 17β-Estradiol on Mitochondrial Calcium Uptake. We recently showed that E2-induced mtROS modulate the growth of estrogen-dependent cells (*4*). Since an increase in the level of mtROS can accelerate Ca^{2+}_{mito} production (*18*), we examined whether E2-induced mtROS were coupled to an increase in $[Ca^{2+}]_{mito}$. Previously, we observed that the peak of E2-induced DNA synthesis occurred at 24 h (*4*), so we measured the level of Ca^{2+}_{mito} after E2 exposure for 24 h. MCF7 breast cancer cells were loaded with rhod-2/AM, a Ca^{2+}-sensitive fluorescent indicator (*19*) that accumulates in mitochondria (*20*). To determine the localization of rhod-2, MCF7 cells were loaded with the mitochondrion-specific probe MitoTracker Green. Cell regions that showed a definite colocalization of these fluorescent probes were used to monitor Ca^{2+}_{mito}.

Interestingly, Ca^{2+}_{mito} uptake did not show an all-or-none response to 17β-estradiol (E2). Instead, the Ca^{2+}_{mito} uptake within a single cell differed between two distinct populations of mitochondria. Thus, the term "high capacity" refers to a $[Ca^{2+}]_{mito}$ of $\geq$0.8 μM, and "low capacity" refers to a $[Ca^{2+}]_{mito}$ in the range of 0.25−0.3 μM. MCF7 cells treated for 24 h with E2 (367 pM) showed an increase in the $[Ca^{2+}]_{mito}$ from a control value of 0.8 $\pm$ 0.011 to 1.1 $\pm$ 0.055 μM (Figure 1A, $P < 0.001$). At 72 h, E2 treatment increased the $[Ca^{2+}]_{mito}$ from a control value of 0.83 $\pm$ 0.015 to 0.97 $\pm$ 0.031 μM (Figure 1A, $P < 0.001$). In contrast, E2 treatment showed no significant change in the corresponding low-capacity mitochondria (Figure 1B) and therefore indicates a functional heterogeneity in mitochondria with respect to E2-induced Ca^{2+}_{mito} uptake. Since high-capacity mitochondria are sensitive while the low-capacity mitochondria are resistant to E2 exposure, the response of high-capacity mitochondria became the focus of further experiments.

To determine whether the ER is involved in the E2-induced uptake of Ca^{2+}_{mito}, MCF7 cells were pretreated for 1 h with the selective ER modulator (SERM) tamoxifen (120 ng/mL). Tamoxifen treatment alone significantly increased the $[Ca^{2+}]_{mito}$ to a value of 1.274 $\pm$ 0.094 μM after 24 h (Figure 1C, $P < 0.001$). The observed tamoxifen-induced increase in $[Ca^{2+}]_{mito}$ is not in agreement with a recent report that showed a decrease in the rate of Ca^{2+}_{mito} uptake in MCF7 cells (*21*). However, the study by Lobaton et al. (*21*) used higher concentrations (micromolar) of tamoxifen, exposed cells for a shorter time period (1 min), and used a different methodology (Ca^{2+}-sensitive photoprotein aequorin). The mechanism of tamoxifen-induced Ca^{2+}_{mito} uptake is not clear. Since tamoxifen alone has been shown to act as an agonist, it is biologically plausible that tamoxifen can modulate the increase in the level of Ca^{2+}_{mito} through an ER genomic signaling pathway. On the basis of the results with tamoxifen alone, we expected that cotreatment with E2 would show an additive accumulation of Ca^{2+}_{mito}. Instead, cotreatment with E2 showed a decrease in $[Ca^{2+}]_{mito}$ almost to the level of the control (0.9 $\pm$ 0.031 μM, Figure 1C). Tamoxifen treatment alone is known to enhance calcium signaling in MCF7 cells and deregulate it (*22*, *23*). It has been known for a long time that tamoxifen alone acts a full agonist, but

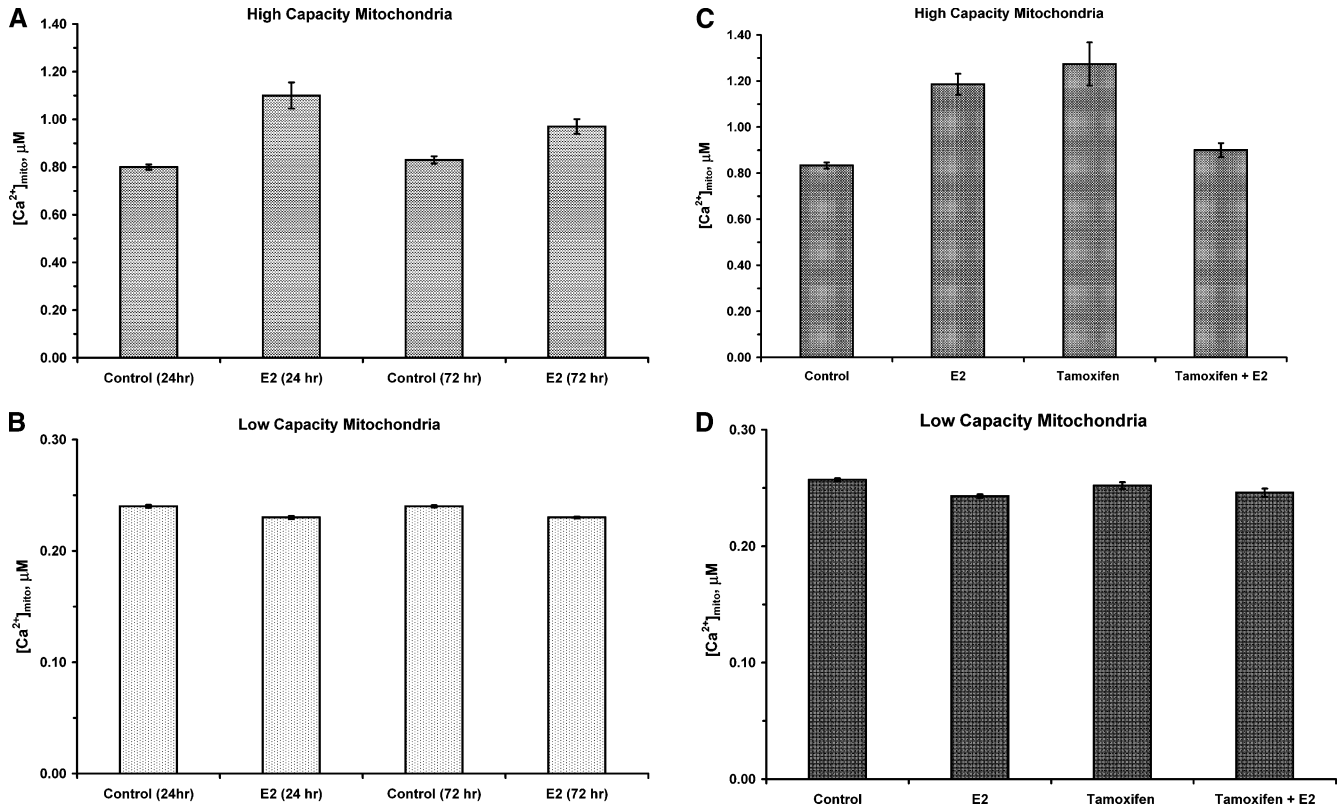

FIGURE 1: Estrogen increases $[Ca^{2+}]_{mito}$ in high-capacity mitochondria. MCF7 cells were cultured on 25 mm diameter coverslips with DMEM/F12 containing 10% charcoal-stripped FBS until they reached approximately 50−60% confluency. Cells were then serum-starved in DMEM/F12 medium for 1 day and then either treated with E2 (100 pg/mL) alone or pretreated for 1 h with tamoxifen followed by E2 treatment for 24 and 72 h. $[Ca^{2+}]_{mito}$ was determined by confocal microscopy as described in Materials and Methods. Two asterisks indicate $P < 0.001$.

as a complete antagonist to a superphysiological dose of estrogen. That excess tamoxifen prevents the action of estrogen is expected, but that the agonist activity of tamoxifen is abolished by 1200 times less estrogen, leading to mutual annihilation of their action, is not. Furthermore, tamoxifen could not be used to elucidate whether E2-induced mtROS is coupled to an increase in $[Ca^{2+}]_{mito}$ because tamoxifen alone can induce cellular oxidative stress (*24*). Although SERMS ICI 182,780 and raloxifene have been shown not to effect $Ca^{2+}{}_{mito}$ uptake (*25*), we could not use them because of their antioxidant activity (*26*, *27*). This limitation prevented further experiments with SERMs because it would be difficult to discern whether a reduction in E2-induced ROS was due to the blockage of the ER or by the antioxidant activity of these compounds.

Effect of Mitochondrial Inhibitors on Estrogen-Induced Calcium Uptake. To confirm that E2 exposure increased the rate of mitochondrial Ca^{2+} uptake, MCF7 cells were cotreated with chemical inhibitors. The mitochondrial respiratory chain blockers rotenone and antimycin A and the mitochondrial ATP synthase blocker oligomycin B are reported to collapse the $\Delta_\Psi m$ and, therefore, prevent $Ca^{2+}{}_{mito}$ uptake (*28*). Rhodamine 6G is a potent inhibitor of oxidative phosphorylation and is reported to block ATP-supported $Ca^{2+}{}_{mito}$ accumulation (*29*). In addition to the use of chemical inhibitors, we used the peptide cyclosporin A which is reported to inhibit $Ca^{2+}{}_{mito}$ uptake through the Ca^{2+} uniporter (*30*). MCF7 cells were pretreated for 1 h with 1 μg/mL rotenone followed by E2 (100 pg/mL) for 24 h in the continued presence of the inhibitor (Figure 2A). Cotreatment with rotenone showed a decrease in $[Ca^{2+}]_{mito}$ from an E2-induced value of 1.186 ± 0.045 to 0.755 ± 0.046 μM ($P < 0.003$, Figure 2A). Antimycin A (46 nM) treatment alone significantly increased the $[Ca^{2+}]_{mito}$ from a control value of 0.833 ± 0.014 to 1.041 ± 0.016 μM ($P < 0.001$, Figure 2A). However, in the presence of antimycin A, we observed a small decrease in the E2-induced $[Ca^{2+}]_{mito}$ from 1.186 ± 0.045 to 1.011 ± 0.015 μM ($P < 0.001$, Figure 2A). MCF7 cells pretreated with oligomycin B (50 pg/mL) for 1 h followed by a 24 h exposure to E2 (Figure 2C) showed a decrease in the $[Ca^{2+}]_{mito}$ from 1.186 ± 0.045 to 1.038 ± 0.018 μM. As shown in Figure 2C, rhodamine 6G (1 μg/mL) treatment alone showed an increase in the $[Ca^{2+}]_{mito}$ from 0.833 ± 0.013 to 0.986 ± 0.092 μM ($P < 0.003$). However, cotreatment of rhodamine 6G with E2 reduced the $[Ca^{2+}]_{mito}$ from an E2-induced value of 1.186 ± 0.045 to 0.988 ± 0.072 μM (Figure 2C). Cyclosporin A (100 ng/mL) treatment alone increased the $[Ca^{2+}]_{mito}$ from a control value of 0.833 ± 0.014 to 1.0439 ± 0.013 μM (Figure 2E). Cotreatment of cyclosporin A and E2 showed a decrease in $[Ca^{2+}]_{mito}$ from 1.186 ± 0.045 to 0.995 ± 0.016 μM ($P < 0.001$, Figure 2E). With the exception of rotenone, none of the mitochondrial blockers were able to completely block the increase in the level of E2-induced mitochondrial Ca^{2+} at 24 h. Since these inhibitors may more effectively block mitochondrial Ca^{2+} uptake at an earlier time point, we measured the $[Ca^{2+}]_{mito}$ after E2 exposure for 30−90 s and observed a unique spatial and temporal increase in the levels of both calcium and ROS. Thus, subsequent experiments were performed at early time points to determine the relationship between mtROS and $Ca^{2+}{}_{mito}$.

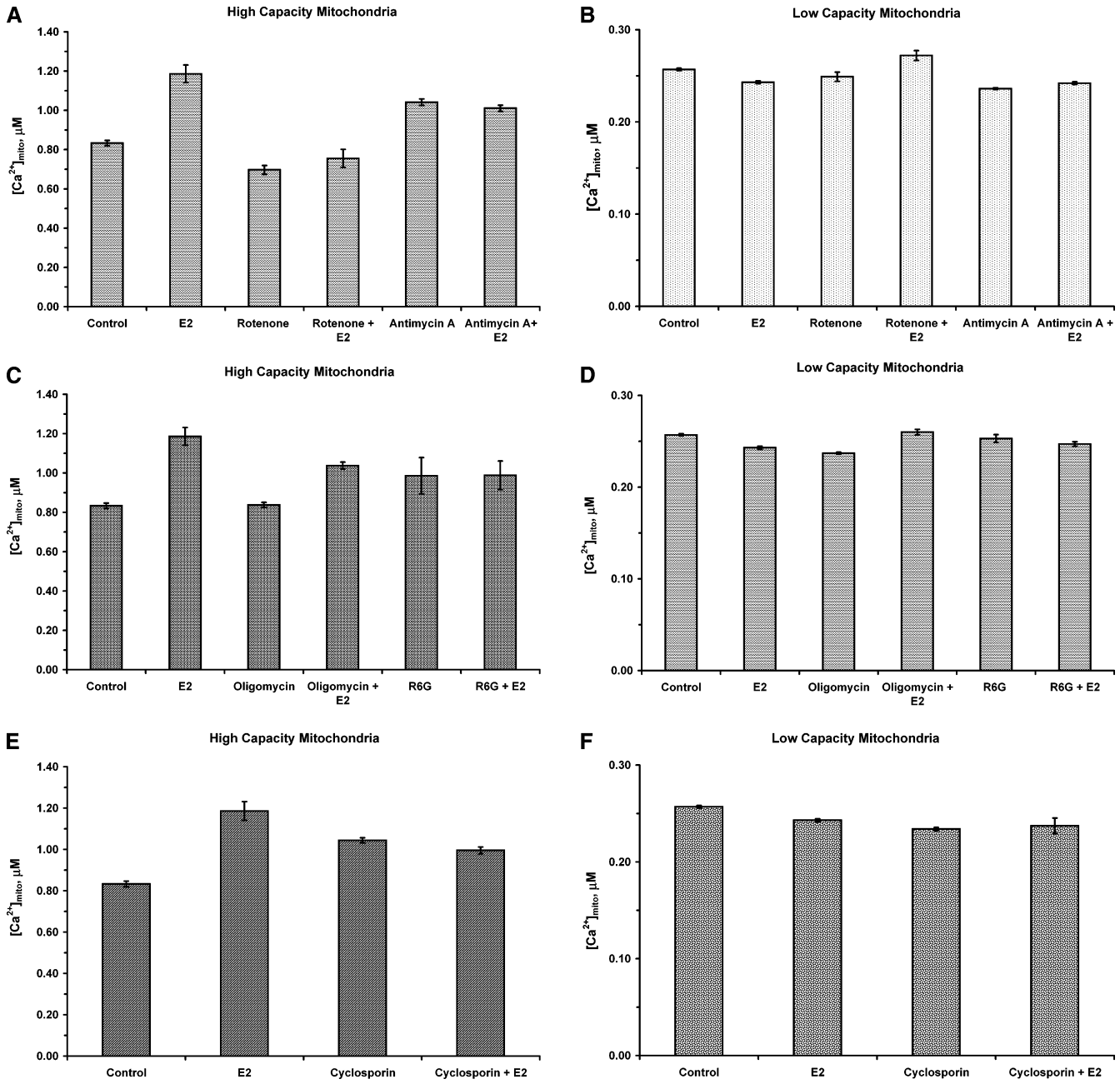

FIGURE 2: Mitochondrial blockers attenuate the estrogen-induced increase in $[Ca^{2+}]_{mito}$ in high-capacity mitochondria. MCF7 cells were cultured as described previously: (A and B) MCF7 cells pretreated for 1 h with rotenone (1 μg/mL), antimycin A (25 ng/mL), oligomycin B (50 pg/mL), rhodamine 6G (1 μg/mL), or cyclosporin A (100 ng/mL) and then exposed to E2. $[Ca^{2+}]_{mito}$ was determined by confocal microscopy as described in Materials and Methods.

Relationship between Reactive Oxygen Species and Calcium. As shown in Figure 3A, the $[Ca^{2+}]_i$ increased approximately 3 min after exposure to E2 (100 and 500 pg/mL). Two different doses of estrogen were used in the measurement of changes in intracellular calcium concentration ($[Ca^{2+}]_i$) because we wanted to determine any saturation or highly significant increases in $[Ca^{2+}]_i$ upon addition of a higher concentration of estrogen (Figure 3A). The level of calcium increased with a slower rate after the second exposure of E2 (500 pg/mL), the concentration of which was 5 times higher than that of the first dose of E2 (100 pg/mL). This indicates that the cellular calcium concentration increase in response to the first E2 exposure is in the proximity of saturation, because we did not observe the proportional increase in calcium concentration by a dose of estrogen that was 5 times higher. To monitor the production of ROS, MCF7 cells were loaded with the fluorophore DCFH-DA. DCFH-DA is a nonfluorescent cell-permeable compound that becomes trapped inside the cell after the acetate group is removed by esterases generating DCFH. In the presence of ROS, DCFH is rapidly oxidized to the highly fluorescent 2′,7′-dichlorofluorescein (DCF) (*31*). We observed a rapid increase in intracellular DCF intensity approximately 1 min from the time of E2 (100 pg/mL) exposure (Figure 3B). It should be noted that a total of 24 individual cells were monitored for changes in DCF intensity, and we therefore displayed a representative sample of individual cell responses to E2 (Figure 3B). The variation observed in both calcium uptake and ROS production among the cells depended on cell density. Cells with less cell−cell contact generated more

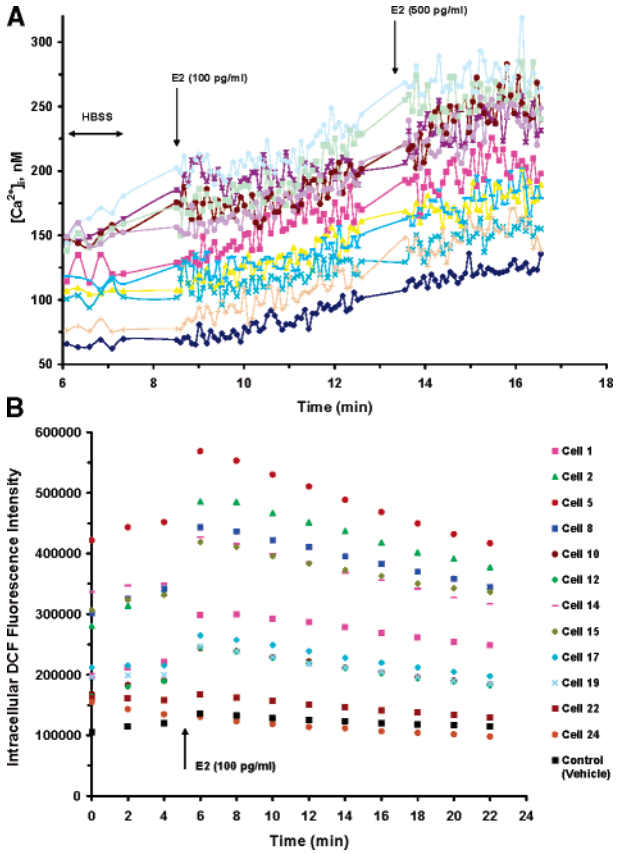

FIGURE 3: Estrogen-induced production of intracellular reactive oxygen species precedes the increase in $[Ca^{2+}]_i$. A total of 24 individual MCF7 cells were monitored for changes in $[Ca^{2+}]_i$ and the level of intracellular ROS when exposed to E2. (A) $[Ca^{2+}]_i$ increased approximately 3 min after exposure to E2 (100 and 500 pg/mL). (B) A time course of DCF intensity monitored in a representative sample from the 24 individual cells when treated with E2 (100 pg/mL). MCF7 cells show a rapid increase in the level of intracellular ROS approximately 1 min from the time of E2 (100 pg/mL) exposure. Each point in the vehicle control is the mean of data from 12 cells.

ROS and calcium uptake than cells with more contacts. This suggests that sparse cells generate more ROS and calcium uptake in response to estrogen because they require it for growth, whereas confluent cells do not need it and consistently exhibited less ROS production and calcium uptake. Our observations are corroborated by another study which showed that the arrest of growth induced by cell confluence ("contact inhibition") is due, at least in part, to a decrease in the steady-state levels of intracellular ROS and the consequent impairment of mitogenic redox signaling (*32*). These results show that E2-induced intracellular ROS precedes the increase in the level of $Ca^{2+}{}_i$. Subsequent experiments were performed to determine whether mtROS and $Ca^{2+}{}_{mito}$ followed a similar temporal pattern.

The colocalization of fluorescent probes DCFH-DA and MitoTracker Deep Red was used to monitor changes in mitochondrial ROS. Our results showed that mitochondrial DCF intensity increased approximately 1 min after E2 exposure (Figure 4A) which correlated with the previous increase in the total intracellular level of ROS. In both panels A and C of Figure 4, we measured the rate of calcium uptake and ROS every 20 s for 5 min in the absence of estrogen (i.e., vehicle alone), and we did not find any change in these cells. The calcium uptake level in mitochondria as well as the mitochondrial ROS level did not change upon addition of the vehicle alone (data not shown). It should be noted again that a total of 24 individual cells were monitored for changes in DCF intensity. Furthermore, we measured the mitochondrial DCF intensity at shorter time intervals (Figure 4B). In cells not treated with estrogen but which received vehicle, we did not see any change in the ROS level with time, whereas upon addition of 100 pg/mL estrogen to the MCF7 cells, we found significant increases in the ROS level with time as early as 20 s from the time of E2 exposure. The changes in DCF and Rhod-2 fluorescence intensities from Figure 4B were quantified as shown in panels A and C of Figure 4. When we monitored the level of $Ca^{2+}{}_{mito}$, we observed an increase in Rhod-2 intensity within 1 min of E2 treatment (Figure 4C) that coincided with the previous increase in DCF intensity. Thus, we monitored earlier $Ca^{2+}{}_{mito}$ levels to determine whether it changed as rapidly (20 s) as that of mtROS. As shown in Figure 4D, E2 markedly increased Rhod-2 intensity in the basal region of the cell after exposure for 90 s. The apical and middle cell regions at 30 and 60 s, respectively, did not show a change in Rhod-2 intensity when compared to control; however, we did observe an increase in DCF intensity (Figure 4D). On the basis of these results, E2-induced mtROS precedes the increase in the level of $Ca^{2+}{}_{mito}$. With respect to Rhod-2 intensity, we observed a spatially distinct distribution of Ca^{2+} in E2-treated MCF7 cells. The basal region showed an increase in Rhod-2 intensity, but the apical and middle regions of the same cells showed no change (Figure 4D).

Biological Response to Estrogen-Induced Calcium. Ca^{2+} is a universal second messenger that can activate the transcription factor CREB which subsequently affects target genes containing the cyclic AMP response element (CRE) in their promoters. Besides CRE, Ca^{2+} signaling can also activate target genes with a serum response element (SRE) or other as yet undefined Ca^{2+} responsive element in their promoters. To determine the genomic effects of E2-induced Ca^{2+} uptake, we screened cells with the nonradioactive human cAMP/Ca^{2+} PathwayFinder gene array (SuperArray) that contains three groups of Ca^{2+} responsive target genes (96 in total): (i) target genes with SRE, (ii) target genes with CRE, and (iii) target genes with undefined elements. E2-induced gene expression was assessed at 6 h because we have shown that mitochondrial blockers reduce the level of expression of early cell cycle genes, resulting in the arrest of E2-dependent cell growth at this time point (*4*). At 6 h, E2 increased the level of expression of the Substance P receptor (NKIR) and transforming growth factor β3 (TGF β3) approximately 2.9- and 3.5-fold, respectively, when compared to control (data not shown). Post-array verification was performed on genes with a significant ($\geq$2-fold) change in expression. Real-time PCR analysis using TaqMan probes for NKIR and TGF b3 did not show a significant change in the level of either gene when compared to control (data not shown). Our findings show that the early E2-induced Ca^{2+} does not alter the expression of these genes involved in calcium signaling pathways.

Since we have shown that E2-induced CREB phosphorylation, transcriptional activity, and binding to the cyclin D1 promoter are all inhibited when the compound is cotreated with rotenone (*4*, *5*), and because we observed that rotenone effectively (100%) blocked the E2-induced increase

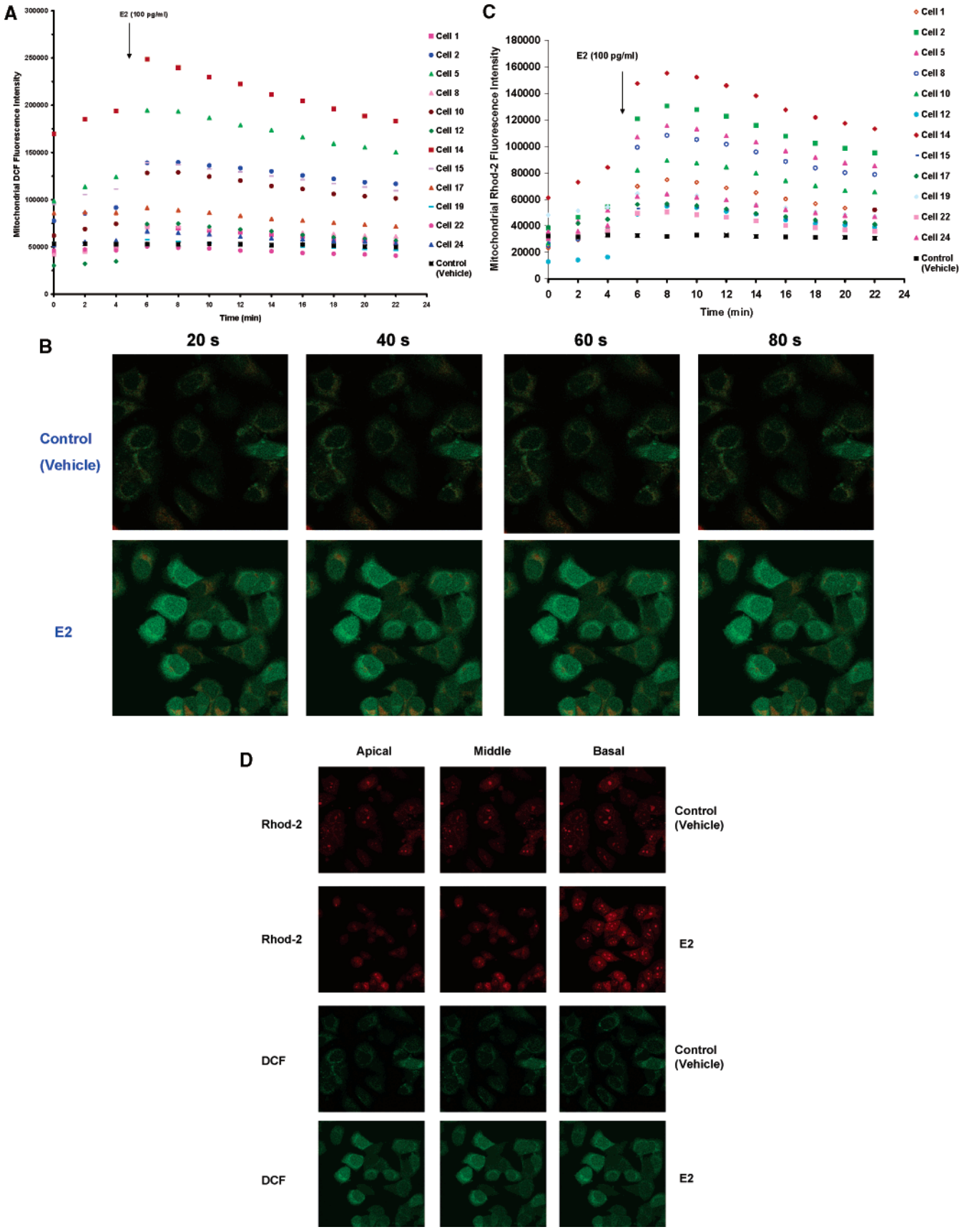

FIGURE 4: Mitochondrial calcium uptake in response to estrogen. A total of 24 individual cells were monitored for changes in mitochondrial DCF intensity. (A) A time course of mitochondrial DCF intensity monitored in a representative sample from the 24 individual cells when treated with E2 (100 pg/mL). Each point in the vehicle control is the mean of data from 12 cells. (B) Confocal images show ROS production over time in a control receiving vehicle (top) and estrogen-treated cells (bottom). Magnification is 63×. Green is DCF, and red is MitoTracker. (C) A time course of rhod-2 intensity monitored in a representative sample from the 24 individual cells when treated with E2 (100 pg/mL). Each point in the vehicle control is the mean of data from 12 cells. (D) Time series of images showing rhod-2 intensity juxtaposed to DCF intensity in the apical, middle, and basal regions of MCF7 cells exposed to E2 (100 pg/mL). Green is DCF, and red is rhod-2. Magnification is 63×.

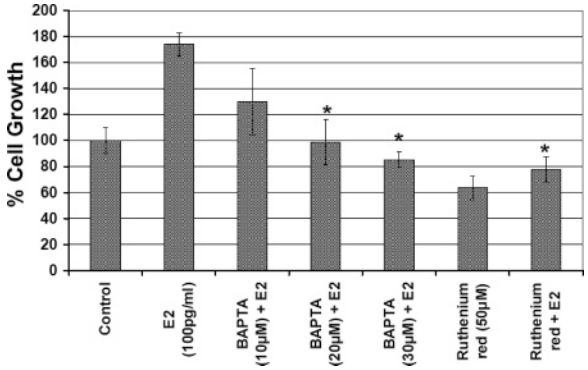

FIGURE 5: Early estrogen-induced Ca^{2+} effects are nongenomic. Pretreatment with BAPTA-AM and ruthenium red inhibits E2-induced growth of MCF7 cells. For cell growth experiments, cells were seeded (3000 cells/well) in 96-well plates, grown for 1 day in 10% FBS DMEM/F12, and serum-starved for 2 days in DMEM/F12, followed by a 1 h pretreatment with BAPTA-AM or ruthenium red. After pretreatment, cells were treated with E2 (100 pg/mL) for 72 h and cell growth was assessed by the SRB assay. Results are expressed as the mean optical density ± the standard deviation of three separate experiments with the control set as 100% cell growth. An asterisk ($P < 0.05$) indicates treatment significantly different from that with E2.

in $[Ca^{2+}]_{mito}$ (Figure 2A), we tested whether E2-induced $Ca^{2+}{}_{mito}$ modulates the growth of estrogen-dependent breast cancer cells. Using the intracellular calcium chelator BAPTA-AM and the $Ca^{2+}{}_{mito}$ uniporter blocker ruthenium red, we evaluated the effect of E2-induced Ca^{2+} on cell growth. E2-induced cell growth was abolished in cells preincubated with 30 μM BAPTA-AM (Figure 5). Pretreatment with ruthenium red (50 μM) also showed inhibition of E2-induced cell growth (Figure 5). Additionally, both BAPTA-AM (20 μM) and ruthenium red (50 μM) induced a complete collapse of the $\Delta\psi m$ (assessed with TMRM, data not shown) and therefore prevented any subsequent uptake of Ca^{2+} into mitochondria. Therefore, the inhibition of E2-induced cell growth by BAPTA-AM and ruthenium red could be attributed to a lack of $Ca^{2+}{}_{mito}$ uptake. Our findings support a significant role for Ca^{2+} in the control of MCF7 cell cycle progression.

DISCUSSION

We have shown that $Ca^{2+}{}_{mito}$ uptake within an individual cell can differ between two distinct populations of mitochondria with respect to their response to E2-induced $Ca^{2+}{}_{mito}$ uptake. Mitochondria that had a $[Ca^{2+}]_{mito}$ of ≥ 0.8 μM were responsive to E2 treatment, while mitochondria with a lower $[Ca^{2+}]_{mito}$ showed no response (Figure 1A,B). Our findings are corroborated by other studies in which similar heterogeneous $Ca^{2+}{}_{mito}$ uptake was observed (*33*−*35*). Since the low-Ca^{2+} capacity mitochondria did not show a response to E2 or to treatment with mitochondrial Ca^{2+} specific blockers, these findings suggest that only high-Ca^{2+} capacity mitochondria are involved in the response to estrogen. Our data suggest that high-Ca^{2+} capacity mitochondria are recruited in response to the new metabolic requirements of E2 stimulation or, as in this case, to promote oxidative signaling. The estrogen-stimulated uptake of Ca^{2+} by high-capacity mitochondria plays a role in cell growth based on our data that showed inhibition of cell growth by the calcium chelator BAPTA and mitochondrial calcium uniporter blocker ruthenium red. Our findings support a significant role for Ca^{2+} in the control of E2-induced MCF7 cell cycle progression. More interestingly, the suppression of E2-induced $Ca^{2+}{}_{mito}$ uptake by the mitochondrial inhibitor rotenone (Figure 2A), which is not known to bind the ER, supports the idea that these effects on $Ca^{2+}{}_{mito}$ uptake and/or mtROS promote oxidative signaling without involving nuclear ER signaling. Mitochondria may coordinate signal transduction pathways that run parallel to nuclear ER signaling. Therefore, we postulate that a subpopulation of mitochondria acts like E2 sensors, potentially allowing forces triggered by altered cytoarchitecture in response to E2 exposure to be transmitted to these organelles, which in turn increases the rate of release of ROS signals to the cytosol.

In the study presented here, we have shown that E2-induced mtROS precedes $Ca^{2+}{}_{mito}$ uptake. The mechanism of $Ca^{2+}{}_{mito}$ uptake in response to E2 is not clear. Although E2 has been shown to increase the level of mitochondrial retention of Ca^{2+} by inhibiting Na-dependent Ca^{2+} efflux (*10*), our data imply that a sufficient amount of E2 would need to cross the plasma membrane and bind to the mitochondrial membrane in 20 s for this mechanism to work, which is not likely to occur in this short amount of time. Under physiological conditions, mitochondria only transiently take up Ca^{2+} released by the proximate endoplasmic reticulum upon stimulation (*36*). ROS have been shown to increase the level of cytosolic Ca^{2+} through the mobilization of intracellular Ca^{2+} stores and/or through the influx of extracellular Ca^{2+} (*37*). Relatively low concentrations of hydroperoxides have also been shown to cause transient changes in $[Ca^{2+}]_i$ (*38*, *39*). These studies in conjunction with our results suggest that a low level of mtROS triggered by E2 exposure stimulates the release of Ca^{2+} from the endoplasmic reticulum and this is taken up by mitochondria.

ER-mediated signaling pathways are considered to support the growth of normal, preneoplastic, and neoplastic cells (*40*−*42*); therefore, we pretreated MCF7 cells with tamoxifen to determine whether the increase in the rate of $Ca^{2+}{}_{mito}$ uptake at 24 h was due to a genomic effect. Even though tamoxifen counteracted E2-induced $Ca^{2+}{}_{mito}$ uptake at 24 h (Figure 1C), it was difficult to conclude whether this effect was a consequence of blocking the ER because tamoxifen is reported to enhance and deregulate calcium signaling in MCF7 cells (*22*, *23*). Moreover, we showed that tamoxifen alone increased the rate of Ca^{2+} uptake to the same level as E2. The use of other SERMS such as ICI 182,780 and raloxifene has already been shown not to affect E2-induced $Ca^{2+}{}_{mito}$ uptake (*43*). Furthermore, several limitations of SERMs made it difficult for us to address the question of whether E2-induced ROS preceded $Ca^{2+}{}_{mito}$ uptake. These limitations are that tamoxifen alone increases the level of cellular oxidative stress (*24*) while ICI 182,780 and raloxifene can act as antioxidants (*26*, *27*).

To understand the mechanism by which mitochondria accumulate Ca^{2+} in response to E2, we treated MCF7 cells with several different mitochondrial calcium blockers. All of the $Ca^{2+}{}_{mito}$ blockers were able to inhibit E2-induced $Ca^{2+}{}_{mito}$ uptake (Figure 2); however, rotenone was the only agent that completely abolished an increase in $[Ca^{2+}]_{mito}$ (Figure 2A). Therefore, we conducted similar experiments at an earlier (30−90 s) time point in an attempt to show that the potency of these inhibitors depended on time. At the early

time point, we observed a unique spatial and temporal increase with respect to E2-induced mitochondrial calcium and mtROS levels. Initially, we observed that E2-induced intracellular ROS preceded the increase in $[Ca^{2+}]_i$ (Figure 3A,B). A more in-depth study of the level of mitochondria revealed that E2 improved ROS production as early as 20 s (Figure 4B), while the calcium response lagged behind at 90 s (Figure 4D). A spatial distinction between mitochondria became apparent when comparing Ca^{2+}_{mito} in the apical, middle, and basal cell regions. Confocal microscopy showed a basal increase in the level of Ca^{2+}_{mito}, while the apical and middle regions showed no change caused by E2 exposure (Figure 4D). Thus, it appears that high-capacity mitochondria are basally located while low-capacity mitochondria are found in the apical and middle regions.

A hierarchy of organ tissue response to E2 has shown that calcium metabolism is the most sensitive followed by epithelial cell growth (*44*). Therefore, we screened Ca^{2+} responsive target genes to determine the genomic effects of E2-induced Ca^{2+} uptake. Initially, the gene array showed that E2 treatment significantly (≥2-fold) increased the response of only two of the 96 calcium sensitive target genes. However, real-time PCR analysis of NKIR and TGF b3 did not show a significant change in the level of either gene when compared to control. These data imply that physiological concentrations of E2 exert nongenomic effects on the cell at this early time point. We have previously shown that E2-induced CREB phosphorylation, transcriptional activity, and binding to the cyclin D1 promoter are suppressed by pretreatment with rotenone (*4, 5*). In the study presented here, rotenone completely blocked the E2-induced increase in the rate of Ca^{2+}_{mito} uptake (Figure 2A). Thus, we studied whether mitochondrion-dependent intracellular calcium signaling modulated E2-induced cell growth. Pretreatment with BAPTA-AM and ruthenium red showed complete inhibition of E2-induced cell growth (Figure 5). In addition, E2-induced DNA synthesis was inhibited by 72% when cells were pretreated with either BAPTA-AM or ruthenium red as measured by the extent of BrdUrd incorporation (data not shown). Although the antiproliferative mechanism for BAPTA-AM and ruthenium red is not clear, our TMRM results showed that these agents collapsed the $\Delta\Psi m$ while E2 treatment alone increased the $\Delta\Psi m$ (data not shown). Mitochondrial calcium uptake depends on $\Delta\Psi m$, and dissipation of the potential provides a way to examine the consequences of Ca^{2+}_{mito} uptake. We have shown recently that E2-mediated ROS production controls promoter activity of cyclin D1 by post-translational modification of calcium sensitive transcription factor CREB (*4*). Thus, our results suggest that E2-induced changes in Ca^{2+}_{mito} and mtROS may be involved in cell cycle progression presumably through the control of early cell cycle genes.

In summary, our data indicate that physiological concentrations of estradiol modulate mitochondrial calcium uptake within 90 s through a nongenomic pathway that is spatially localized to the basal region of the cell. Interestingly, this calcium response lagged behind the induction of mtROS. The conventional paradigm of estrogen action is based on binding to its receptors, ERα/β, which initiates transcription by binding to estrogen response elements (EREs) of genes. However, the absence of E2-induced calcium sensitive gene expression at an early time point underscores the critical role of nongenomic E2 effects associated with Ca^{2+} signaling in cell cycle progression. We suggest that these rapid E2-induced changes in mtROS and Ca^{2+}_{mito} result in post-translational modifications involved in early G1 phase cell cycle progression. Thus, targeting mitochondria to disrupt communication between mitochondria and Ca^{2+} signaling pathways provides the basis for a novel anticancer strategy for the treatment of estrogen-dependent breast cancer.

REFERENCES

1. Benten, W. P., Stephan, C., Lieberherr, M., and Wunderlich, F. (2001) Estradiol signaling via sequestrable surface receptors, *Endocrinology 142*, 1669−1677.
2. Guo, Z., Krucken, J., Benten, W. P., and Wunderlich, F. (2002) Estradiol-induced nongenomic calcium signaling regulates genotropic signaling in macrophages, *J. Biol. Chem. 277*, 7044−7050.
3. Felty, Q., and Roy, D. (2005) Estrogen, mitochondria, and growth of cancer and non-cancer cells, *J. Carcinog. 4*, 1.
4. Felty, Q., Singh, K. P., and Roy, D. (2005) Estrogen-induced G_1/S transition of G_0-arrested estrogen-dependent breast cancer cells is regulated by mitochondrial oxidant signaling, *Oncogene 24*, 4883−4893.
5. Felty, Q., Xiong, W. C., Sun, D., Sarkar, S., Singh, K. P., Parkash, J., and Roy, D. (2005) Estrogen-induced mitochondrial reactive oxygen species as signal-transducing messengers, *Biochemistry 44*, 6900−6909.
6. Lu, K. P., and Means, A. R. (1993) Regulation of the cell cycle by calcium and calmodulin, *Endocr. Rev. 14*, 40−58.
7. Montero, M., Lobaton, C. D., Hernandez-Sanmiguel, E., Santodomingo, J., Vay, L., Moreno, A., and Alvarez, J. (2004) Direct activation of the mitochondrial calcium uniporter by natural plant flavonoids, *Biochem. J. 384*, 19−24.
8. Gunter, T. E., Buntinas, L., Sparagna, G., Eliseev, R., and Gunter, K. (2000) Mitochondrial calcium transport: Mechanisms and functions, *Cell Calcium 28*, 285−296.
9. Morkuniene, R., Jekabsone, A., and Borutaite, V. (2002) Estrogens prevent calcium-induced release of cytochrome *c* from heart mitochondria, *FEBS Lett. 521*, 53−56.
10. Horvat, A., Petrovic, S., Nedeljkovic, N., Martinovic, J. V., and Nikezic, G. (2000) Estradiol affect Na-dependent Ca^{2+} efflux from synaptosomal mitochondria, *Gen. Physiol. Biophys. 19*, 59−71.
11. Nilsen, J., and Diaz, B. R. (2003) Mechanism of estrogen-mediated neuroprotection: Regulation of mitochondrial calcium and Bcl-2 expression, *Proc. Natl. Acad. Sci. U.S.A. 100*, 2842−2847.
12. Lobaton, C. D., Vay, L., Hernandez-Sanmiguel, E., Santodomingo, J., Moreno, A., Montero, M., and Alvarez, J. (2005) Modulation of mitochondrial Ca^{2+} uptake by estrogen receptor agonists and antagonists, *Br. J. Pharmacol. 145*, 862−871.
13. Roy, D., Parkash, J., and Narayan, S. (2005) Genetics and Bioenergetics of Mitochondria Influencing the Etiology and Pharmacology of Steroidal Hormones, *Curr. Pharmacogenomics 2*, 379−390.
14. Parkash, J., Chaudhry, M. A., and Rhoten, W. B. (2004) Ca^{2+} sensing receptor activation by $CaCl_2$ increases $[Ca^{2+}]_i$ resulting in enhanced spatial interactions with calbindin-D28k protein, *Int. J. Mol. Med. 13*, 3−11.
15. DuMond, J. W., Jr., Singh, K. P., and Roy, D. (2001) The biphasic stimulation of proliferation of Leydig cells by estrogen exposure, *Int. J. Oncol. 18*, 623−628.
16. Skehan, P., Storeng, R., Scudiero, D., Monks, A., McMahon, J., Vistica, D., Warren, J. T., Bokesch, H., Kenney, S., and Boyd, M. R. (1990) New colorimetric cytotoxicity assay for anticancer-drug screening, *J. Natl. Cancer Inst. 82*, 1107−1112.
17. Huang, S. G. (2002) Development of a high throughput screening assay for mitochondrial membrane potential in living cells, *J. Biomol. Screening 7*, 383−389.
18. Starkov, A. A., Chinopoulos, C., and Fiskum, G. (2004) Mitochondrial calcium and oxidative stress as mediators of ischemic brain injury, *Cell Calcium 36*, 257−264.
19. Minta, A., Kao, J. P., and Tsien, R. Y. (1989) Fluorescent indicators for cytosolic calcium based on rhodamine and fluorescein chromophores, *J. Biol. Chem. 264*, 8171−8178.
20. Boitier, E., Rea, R., and Duchen, M. R. (1999) Mitochondria exert a negative feedback on the propagation of intracellular Ca^{2+} waves in rat cortical astrocytes, *J. Cell Biol. 145*, 795−808.

21. Lobaton, C. D., Vay, L., Hernandez-Sanmiguel, E., Santodomingo, J., Moreno, A., Montero, M., and Alvarez, J. (2005) Modulation of mitochondrial Ca^{2+} uptake by estrogen receptor agonists and antagonists, *Br. J. Pharmacol. 145*, 862−871.
22. Jain, P. T., and Trump, B. F. (1997) Tamoxifen induces deregulation of [Ca^{2+}] in human breast cancer cells, *Anticancer Res. 17*, 1167−1174.
23. Zhang, W., Couldwell, W. T., Song, H., Takano, T., Lin, J. H., and Nedergaard, M. (2000) Tamoxifen-induced enhancement of calcium signaling in glioma and MCF-7 breast cancer cells, *Cancer Res. 60*, 5395−5400.
24. Schiff, R., Reddy, P., Ahotupa, M., Coronado-Heinsohn, E., Grim, M., Hilsenbeck, S. G., Lawrence, R., Deneke, S., Herrera, R., Chamness, G. C., Fuqua, S. A., Brown, P. H., and Osborne, C. K. (2000) Oxidative stress and AP-1 activity in tamoxifen-resistant breast tumors in vivo, *J. Natl. Cancer Inst. 92*, 1926−1934.
25. Lobaton, C. D., Vay, L., Hernandez-Sanmiguel, E., Santodomingo, J., Moreno, A., Montero, M., and Alvarez, J. (2005) Modulation of mitochondrial Ca^{2+} uptake by estrogen receptor agonists and antagonists, *Br. J. Pharmacol*.
26. Arteaga, E., Villaseca, P., Bianchi, M., Rojas, A., and Marshall, G. (2003) Raloxifene is a better antioxidant of low-density lipoprotein than estradiol or tamoxifen in postmenopausal women in vitro, *Menopause 10*, 142−146.
27. Hermenegildo, C., Garcia-Martinez, M. C., Tarin, J. J., and Cano, A. (2002) Inhibition of low-density lipoprotein oxidation by the pure antiestrogens ICI 182780 and EM-652 (SCH 57068), *Menopause 9*, 430−435.
28. Budd, S. L., and Nicholls, D. G. (1996) Mitochondria, calcium regulation, and acute glutamate excitotoxicity in cultured cerebellar granule cells, *J. Neurochem. 67*, 2282−2291.
29. Gear, A. R. (1974) Rhodamine 6G. A potent inhibitor of mitochondrial oxidative phosphorylation, *J. Biol. Chem. 249*, 3628−3637.
30. Montero, M., Lobaton, C. D., Gutierrez-Fernandez, S., Moreno, A., and Alvarez, J. (2004) Calcineurin-independent inhibition of mitochondrial Ca^{2+} uptake by cyclosporin A, *Br. J. Pharmacol. 141*, 263−268.
31. Swift, L. M., and Sarvazyan, N. (2000) Localization of dichlorofluorescin in cardiac myocytes: Implications for assessment of oxidative stress, *Am. J. Physiol. 278*, H982−H990.
32. Pani, G., Colavitti, R., Bedogni, B., Anzevino, R., Borrello, S., and Galeotti, T. (2000) A redox signaling mechanism for density-dependent inhibition of cell growth, *J. Biol. Chem. 275*, 38891−38899.
33. Collins, T. J., Lipp, P., Berridge, M. J., and Bootman, M. D. (2001) Mitochondrial Ca^{2+} uptake depends on the spatial and temporal profile of cytosolic Ca^{2+} signals, *J. Biol. Chem. 276*, 26411−26420.
34. Collins, T. J., Berridge, M. J., Lipp, P., and Bootman, M. D. (2002) Mitochondria are morphologically and functionally heterogeneous within cells, *EMBO J. 21*, 1616−1627.
35. Monteith, G. R., and Blaustein, M. P. (1999) Heterogeneity of mitochondrial matrix free Ca^{2+}: Resolution of Ca^{2+} dynamics in individual mitochondria in situ, *Am. J. Physiol. 276*, C1193−C1204.
36. Rizzuto, R., Brini, M., Murgia, M., and Pozzan, T. (1993) Microdomains with high Ca^{2+} close to IP3-sensitive channels that are sensed by neighboring mitochondria, *Science 262*, 744−747.
37. Renard, D. C., Seitz, M. B., and Thomas, A. P. (1992) Oxidized glutathione causes sensitization of calcium release to inositol 1,4,5-trisphosphate in permeabilized hepatocytes, *Biochem. J. 284* (Part 2), 507−512.
38. Hoyal, C. R., Thomas, A. P., and Forman, H. J. (1996) Hydroperoxide-induced increases in intracellular calcium due to annexin VI translocation and inactivation of plasma membrane Ca^{2+}-ATPase, *J. Biol. Chem. 271*, 29205−29210.
39. Livingston, F. R., Lui, E. M., Loeb, G. A., and Forman, H. J. (1992) Sublethal oxidant stress induces a reversible increase in intracellular calcium dependent on NAD(P)H oxidation in rat alveolar macrophages, *Arch. Biochem. Biophys. 299*, 83−91.
40. DuMond, J. W., Jr., Singh, K. P., and Roy, D. (2001) Regulation of the growth of mouse Leydig cells by the inactive stereoisomer, 17α-estradiol: Lack of correlation between the elevated expression of ERα and difference in sensitivity to estradiol isomers, *Oncol. Rep. 8*, 899−902.
41. Welshons, W. V., Thayer, K. A., Judy, B. M., Taylor, J. A., Curran, E. M., and Vom Saal, F. S. (2003) Large effects from small exposures. I. Mechanisms for endocrine-disrupting chemicals with estrogenic activity, *Environ. Health Perspect. 111*, 994−1006.
42. Roy, D., and Cai, Q. (2002) Estrogen, immunoactivation, gene damage, and development of breast, endometrial, ovarian, prostate, and testicular cancers, *Recent Res. Dev. Steroid Biochem. Mol. Biol. 3*, 1−32.
43. Lobaton, C. D., Vay, L., Hernandez-Sanmiguel, E., Santodomingo, J., Moreno, A., Montero, M., and Alvarez, J. (2005) Modulation of mitochondrial Ca^{2+} uptake by estrogen receptor agonists and antagonists, *Br. J. Pharmacol*.
44. Barbieri, R. L. (1992) Hormone treatment of endometriosis: The estrogen threshold hypothesis, *Am. J. Obstet. Gynecol. 166*, 740−745.

BI051855X